DFT ^{2}H quadrupolar coupling constants of ruthenium complexes: a good probe of the coordination of hydrides in conjuction with experiments

Iker del Rosal,[a] Torsten Gutmann,[d] Laurent Maron,[a] Franck Jolibois,[a] Bruno Chaudret,[b] Bernadeta Walaszek,[c] Hans-Heinrich Limbach,[c] Romuald Poteau*[a] and Gerd Buntkowsky*[d]

Received 10th December 2008, Accepted 2nd April 2009
First published as an Advance Article on the web 5th May 2009
DOI: 10.1039/b822150b

Transition metal (TM) hydrides are of great interest in chemistry because of their reactivity and their potential as catalysts for hydrogenation reactions. ^{2}H solid-state NMR can be used in order to get information about the local environment of hydrogen atoms, and more particularly the coordination mode of hydrides in such complexes. In this work we will show that it is possible to establish at the level of density functional theory (DFT) a viable methodological strategy that allows the determination of ^{2}H NMR parameters, namely the quadrupolar coupling constant (C_Q) respectively the quadrupolar splitting ($\Delta\nu_Q$) and the asymmetry parameter (η_Q). The reliability of the method (B3PW91-DFT) and basis set effects have been first evaluated for simple organic compounds (benzene and fluorene). A good correlation between experimental and theoretical values is systematically obtained if the large basis set cc-pVTZ is used for the computations. ^{2}H NMR properties of five mononuclear ruthenium complexes (namely $Cp^*RuD_3(PPh_3)$, $Tp^*RuD(THT)_2$, $Tp^*RuD(D_2)(THT)$ and $Tp^*RuD(D_2)_2$ and $RuD_2(D_2)_2(PCy_3)_2$) which exhibit different ligands and hydrides involved in different coordination modes (terminal-H or η^2-H_2), have been calculated and compared to previous experimental data. The results obtained are in excellent agreement with experiments. Although ^{2}H NMR spectra are not always easy to analyze, assistance by quantum chemistry calculations allows unambiguous assignment of the signals of such spectra. As far as experiments can be achieved at very low temperatures in order to avoid dynamic effects, this hybrid theoretical/experimental tool may give useful insights in the context of the characterization of ruthenium surfaces or nanoparticles with solid-state NMR.

1. Introduction

Ruthenium and its derivatives consist an important class of catalysts. They are involved in hydrogenolysis reactions,[1] olefin metathesis[2] and the Fischer–Tropsch reaction.[3,4] Today there is a growing interest to synthesize ruthenium complexes for catalytic reactions and ruthenium nanoparticles which have importance in current material science.[5–8] Due to their physical and chemical properties, resulting from surface or quantum size effects,[9] their potential applications range from magnetic devices to catalysis and selective gas detection.[10] To understand the properties of these catalysts on the molecular level, a thorough characterization with spectroscopic techniques is mandatory. Here in particular ^{2}H solid-state NMR[8] studies, which may reveal both the structure and dynamics of the catalyst and possibly the catalyst substrate complex, are of interest.[11–16] The interpretation of these data necessitates reference data obtained by theoretical modelling on the level of quantum chemistry. However, due to rather scarce theoretical studies of ^{2}H NMR properties of TM compounds in general and ruthenium complexes in particular, there is currently still a lack of reliable reference data and computational methodology. Thus, calculations performed on well-defined experimental systems are important for validating the computational methodology. After confirmation of the accuracy of theoretical methods, the computations could thus contribute to secure the attribution of spectroscopic information in the case where assignment cannot be fully achieved by experimental means or in the structural interpretation of the NMR data. This collaborative experimental/computational calibration and validation is essential before exploring species like organometallic nanoparticles, whose structure cannot be characterized at the same level of accuracy as well-defined molecular species.

Following this line of reasoning, we recently started to study experimentally a set of ruthenium model complexes with well defined structure with ^{2}H solid-state NMR spectroscopy,

[a] *Université de Toulouse; INSA, UPS; LPCNO, IRSAMC; 135 avenue de Rangueil, F-31077 Toulouse, France and CNRS, UMR 5215 (IRSAMC), F-31077 Toulouse, France. E-mail: romuald.poteau@univ-tlse3.fr*
[b] *Université de Toulouse; UPS, CNRS; LCC, 205 route de Narbonne, F-31077 Toulouse, France. E-mail: bruno.chaudret@lcc-toulouse.fr*
[c] *Institut für Physikalische und Theoretische Chemie, Freie Universität Berlin, Takustr. 3, D-14195 Berlin, Germany. E-mail: limbach@chemie.fu-berlin.de*
[d] *Institut für Physikalische Chemie, Friedrich Schiller Universität Jena, Helmholtzweg 4, D-07743 Jena, Germany. E-mail: gerd.buntkowsky@uni-jena.de*

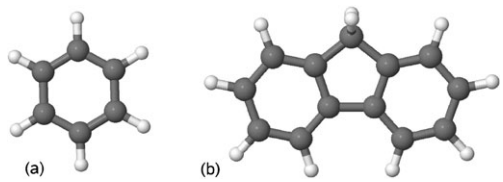

Fig. 1 (a) Benzene; (b) fluorene.

whose experimental NMR data can serve as experimental data base for the calculations.[17] Owing to their computational efficacy, density functional theory (DFT) based calculation techniques are of particular interest. They were successfully applied to the calculations of NMR parameters of various compounds, such as chemical shifts in transition metal complexes,[18–21] quadrupolar interactions in vanadium compounds,[22–24] as well as other studies in the context of hydrogen bonds[25–27] and have shown that DFT is a complementary analytical tool, provided that dynamical effects are well taken into account.[28,29] In the present work, we are particularly interested in elucidating the coordination mode of hydrides in TM complexes. This can be experimentally reached by means of ^{1}H liquid-state NMR or ^{2}H solid-state NMR, after deuterium isotopic substitution.

As a preliminary step, we validate the accuracy of our calculation method and evaluate basis set size effects for simple compounds where experimental ^{2}H solid-state NMR data were available, namely benzene and fluorene (Fig. 1). According to the work of Bailey, who compared the experimental and calculated quadrupolar interaction parameters (quadrupolar coupling constant C_Q and asymmetry of the electric field gradient (EFG) tensor η_Q) at the B3LYP/6-31G(*df*,3*p*) level of theory,[30] calculations of the ^{2}H NMR parameters (quadrupolar splitting $\Delta\nu_Q$ and asymmetry of the electric field gradient (EFG) tensor η_Q) at the PBE0/B3PW91 level of theory were carried out, employing different sized basis sets. Initially, the theoretical results for benzene were compared with the experimental data for bulk benzene-d_6.[31] In this case the bulk benzene-d_6 acts as model for the carbon-deuterium (C–D) binding situation in solid benzen. For the fluorene, acting as model for different C–D binding situations (CD and CD_2) in solids, $\Delta\nu_Q$ values from ^{2}H NMR single crystal measurements[32] were used for the comparision.

The calculations on these two systems helped us to develop an efficient and reliable calculation strategy of the ^{2}H NMR parameters. This strategy is then applied to the calculation of the ^{2}H NMR parameters of five mononuclear ruthenium complexes synthesized by some of us.[17,33] They exhibit different C–D and also ruthenium–deuterium (Ru–D) binding situations of the deuterons and model all reasonably possible hydrogen binding situations of mononuclear ruthenium complexes. The comparison between the caculated parameters and the experimental ones,[17] determined by a combination of MAS and low temperature ^{2}H measurements, enables to elucidate the bonding of deuterium atoms in mononuclear ruthenium complexes. These investigations form the basis for the calculation of ruthenium clusters which picture models for ruthenium nanoparticles.

2. Methodological details

2.1 Mononuclear ruthenium complexes

In recent papers we have reported about the synthesis and experimental study of the ^{2}H-NMR quadrupolar interaction of a series of mononuclear ruthenium complexes with different ligands.[17,33] Our main goal in the present paper is the quantum chemical calculation of the quadrupolar parameters C_Q and η_Q and their comparison with experimental values. The quadrupolar parameters were calculated for the deuterons in three trispyrazolylborate (Tp*) ruthenium complexes with one deuterium and optionally one or two D_2 groups (Fig. 2a to 2c), in a cyclopentadienyl (Cp*) ruthenium complex with three deuteriums (Fig. 2d), and finally in a tricyclohexylphosphin (PCy_3) ruthenium complex with two deuteriums and two D_2 groups (Fig. 2e). The DFT optimized geometries are given in Fig. 3. In particular we wanted to corroborate the experimental finding that there are characteristic quadrupolar coupling constants for ruthenium bound terminal-D and η^2-D_2 ligands. For verification of our calculations, the quadrupolar properties for C-D deuterons were calculated as well.

2.2 Quadrupolar splitting and asymmetry parameter

The basic theory of the quadrupolar interaction of ^{2}H is well-documented[34] and only briefly summarized here. Deuterium has a nuclear spin of $I = 1$. It possesses a quadrupolar moment which is in the range of $Q = 0.00286$ barns. This quadrupolar moment of the deuterium can interact with the electric field gradient arisen at these sites. The energy of this interaction is related to the quadrupolar splitting $\Delta\nu_Q$ which can be measured directly by solid-state NMR spectroscopy, whereas the asymmetry parameter η_Q describes the deviation of the EFG tensor from its cylindric symmetry. A general theoretical description of the quadrupolar interaction is given by the first-order quadrupolar Hamiltonian

$$\hat{H}_Q^{(1)} = \frac{eQV_{33}}{2I(2I-1)\hbar}\frac{1}{2}(3\cos^2\beta - 1 - \eta_Q\sin^2\beta\cos 2\alpha)\left(\frac{3}{2}\hat{I}_z^2 - \frac{I(I+1)}{2}\right) \quad (1)$$

where V_{33} express the largest principal component of the EFG tensor, Q is the quadrupolar moment, e the electronic charge,

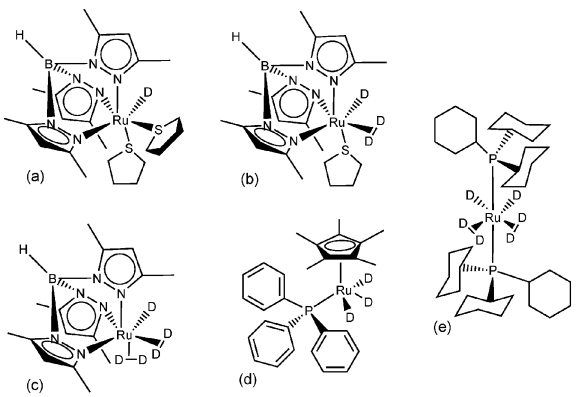

Fig. 2 (a) $Tp^*RuD(THT)_2$; (b) $Tp^*RuD(D_2)(THT)$; (c) $Tp^*RuD(D_2)_2$; (d) $Cp^*RuD_3(PPh_3)$; (e) $RuD_2(D_2)_2(PCy_3)_2$.

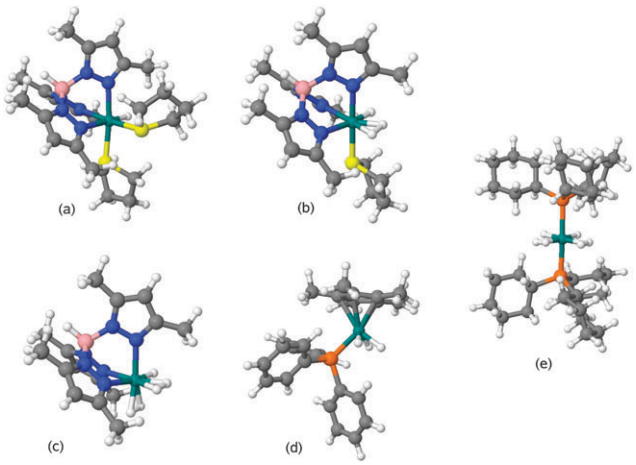

Fig. 3 Optimized structures by 6-31G(d,p) of (a) $Tp^*RuD(THT)_2$; (b) $Tp^*RuD(D_2)(THT)$; (c) $Tp^*RuD(D_2)_2$; (d) $Cp^*RuD_3(PPh_3)$; (e) $RuD_2(D_2)_2(PCy_3)_2$.

$\hbar$ the Planck constant in units of 2π and α and β are the azimuth and polar angle of the quadrupolar principal axes system with respect to the external magnetic field. Inserting the nuclear spin $I = 1$ of the ^2H nucleus and introducing the quadrupolar frequency ν_Q, which depends on the polar angles α and β, gives the following expression (eqn (2)) for the quadrupolar Hamiltonian of a deuteron:

$$\hat{H}_Q^{(1)} = 2\pi\nu_Q\left(\hat{I}_z^2 - \frac{2}{3}\right). \quad (2)$$

DFT calculations allow the computation of the tensor elements V_{ij} of the EFG tensor *via* the electronic density ϱ_e at the ^2H center (eqn (3)).

$$V_{ij} = \int d^3s\varrho_e \frac{3s_is_j - \delta_{ij}s^2}{s^5} \quad (3)$$

To calculate the quadrupolar interaction parameters from the EFG this tensor has to be diagonalized. The quadrupolar coupling constant C_Q and the asymmetry parameter η_Q are then calculated according to eqn (4) and (5).

$$C_Q = \frac{eQV_{33}}{h} \quad (4)$$

$$\eta_Q = \frac{|V_{22}| - |V_{11}|}{|V_{33}|} \quad (5)$$

where V_{11}, V_{22}, V_{33} express the principal components of the EFG tensor with $|V_{11}| \leq |V_{22}| \leq |V_{33}|$. The principal components are initially calculated in atomic units (a.u.). Here the value of eQ/h is 672 kHz/a.u. for deuterium ($Q = 0.00286$ barns for ^2H, after ref. 35). For comparison to experimental spectra these values are converted as

$$C_Q\,(\text{kHz}) = 672 \times V_{33}(\text{a.u.}). \quad (6)$$

The experimentally observable quadrupolar splitting $\Delta\nu_Q$ is related to the quadrupolar coupling constant C_Q according to eqn (7) in case of deuterons.[36]

$$\Delta\nu_Q = \tfrac{3}{4}C_Q \quad (7)$$

The direct conversion from atomic units becomes

$$\Delta\nu_Q = \tfrac{3}{4} \times 672 \times V_{33} = 504 \times V_{33}. \quad (8)$$

2.3 DFT calculations

All DFT calculations were performed with Gaussian03.[37] Geometries were fully optimized in gas phase without symmetry constraints, employing the PBE0[38] functional before calculating EFG tensors. This choice of functional was initially motivated by calculations performed on small magnetic Ru_n clusters, which showed that PBE0 gives the ground-state magnetic moment, bond length, and dissociation energy of Ru_2 in good agreement with experiment and high-level quantum chemistry calculations. It also seems to be a good compromise for suitably describing Ru_3 clusters[39] and its ability to properly describe the geometrical features of organometallic clusters has been proven.[21] Calculations of vibrational frequencies were systematically done in order to characterize the nature of stationary points. The Stuttgart effective core potential[40] and its associated basis set was considered for ruthenium. For the other elements (H, C, O, and P) Pople's double-ζ basis set 6-31G(d,p)[41,42] was used. The calculations of the EFG tensors were done using the B3PW91 functional[43–49] and the Stuttgart effective core potential for Ru, augmented with a polarization function ($\zeta_f = 1.235$). For the other elements (H, C, O, and P) (i) Dunning's correlation consistent basis set cc-pVTZ[50,51] and (ii) Poples double-ζ, respectively triple-ζ basis sets 6-31G(d,p) and 6-311G(d,p) were used. We have proved on some test cases that quadrupolar coupling constants calculated on triple-ζ and double-ζ basis sets' geometries differ by less than 2%, owing to the local character of this property. Due to the large dimension of some TM complexes we have considered that performing geometry optimizations and EFG tensor calculations in the same expensive triple-ζ quality basis set brings no significant enhancement of the results.

3. Results and discussion

3.1 Simple organic compounds

The results of the DFT calculations for the simple molecules benzene and fluorene (Fig. 1) are reported in Table 1 together with experimental data from the literature.[31,32] For all these compounds, the calculated asymmetry parameter η_Q is very close to zero, which results of the axial symmetry of the covalent C–D bonds exhibited in these compounds.

While the calculated η_Q value for each several molecule is almost insensitive to the basis set, the calculated quadrupolar coupling constant C_Q slightly differs between the double-ζ quality 6-31G(*d,p*) basis set and the triple-ζ quality basis sets 6-311G(*d,p*) respectively cc-pVTZ. The difference between the values obtained with the three basis sets is small, but we observe systematically that the results obtained with the triple-ζ 6-311G(*d,p*) basis set are less consistent with respect to experiments than those obtained with the two other basis sets.

Although the theoretical C_Q value is overestimated by *ca.* 10 kHz with respect to the experimental data with the cc-pVTZ basis set, the quality of the calculation is sufficient

Table 1 Comparison of basis sets effect on C_Q, $\Delta\nu_Q$ (in kHz) and η_Q for benzene and fluorene. $\Delta\nu_Q$ is calculated from C_Q according to eqn (7). 6-311G(*d,p*) and cc-pVTZ values are calculated for the optimized 6-31G(*d,p*) geometry

Basis set	6-31G(d,p)			6-311G(d,p)			cc-pVTZ			Experimental	
Parameters	C_Q	$\Delta\nu_Q$	η_Q	C_Q	$\Delta\nu_Q$	η_Q	C_Q	$\Delta\nu_Q$	η_Q	$\Delta\nu_Q$	η_Q
Benzene[a]											
C–D	199	150	0.07	207	156	0.07	194	145	0.06	~136	~0.04
Fluorene[b]											
C–D (CD)	200	150	0.07	208	156	0.07	194	146	0.07	~135	~0.05
C–D (CD_2)	189	142	0.02	196	147	0.02	184	138	0.02	~126	~0.02

[a] Experimental values: Ref. 31. [b] Ref. 32.

to properly differentiate between deuterons in C–D bonds with different bonding situations like CD or CD_2. The difference between calculated $\Delta\nu_Q$ values for CD and CD_2 is indeed 8 kHz, in excellent agreement with the experimental data (9 kHz). The asymmetry parameters are also in line with the experimental results. These simple calculations show that it is possible to distinguish between different C–D bonding situations with our calculation method, which seems promising. Its ability to also characterize metal–deuterium bonding situations like Ru–D or Ru–D_2 is considered in the next sections. This is a more difficult problem due to shallow potential energy surfaces which involve the fluxionality of such organometallic complexes. In other words, DFT calculations, performed at 0 K, must preferentially be compared to experiments performed at sufficiently low temperatures so that the experimental values can be considered as the rigid limit.

3.2 Cp* ruthenium complex

The Cp*$RuD_3(PPh_3)$ complex exhibits an η^5-cyclopentadienyl and a triphenylphosphine ligand coordinated to the ruthenium atom, as well as three terminal deuterons (Fig. 3d). According to the optimized geometry, all Ru–D distances are similar (1.589 Å, 1.579 Å and 1.595 Å), with rather large D–D distances (1.668 Å and 1.694 Å). As can be seen in Table 2, the quadrupolar coupling constant C_Q calculated for the Cp*$RuD_3(PPh_3)$ complex does not change significantly according to the basis set. The relative difference does not exceed 10% between the 6-31G(*d,p*), 6-311G(*d,p*) and cc-pVTZ basis sets. Considering the experimental quadrupolar splitting $\Delta\nu_Q$ at 90 K obtained for Ru–D, the best agreement is observed with the cc-pVTZ basis set (73.1 kHz *vs.* 70 kHz).

The quadrupolar splitting of 70–78 kHz is attributed to the Ru–D bonding, whereas the quadrupolar splitting in the range of 120–140 kHz can be related to the deuterium atoms involved in C–D bonds of the deuterated ligands.[34] There is a very good correlation between theoretical and experimental $\Delta\nu_Q$ values. The quadrupolar splitting for Ru–D is calculated to be 73 kHz employing the cc-pVTZ basis set, which leads to the most accurate results (exp. 70 kHz). It must be underlined that $\Delta\nu_Q$ calculated for C–D in the ruthenium complexes employing the cc-pVTZ basis set is almost identical to those calculated for the simple compounds (benzene and fluorene) in the same basis set (Table 1). This observation shows that for a given quadrupolar nucleus, in our case the deuterium, only the atoms of the first coordination sphere of this nucleus have a large influence on the quadrupolar coupling. The asymmetry parameter η_Q for all calculated bonds is close to zero which refers to the axial symmetry of bonds in the vicinity of the deuteron. The EFG tensors at deuteron centers are shown in Fig. 4. The axial symmetry is obvious, in relation with small values of the asymmetry parameter η_Q. This parameter is indeed expected to be close to 0 due to the approximate cylindrical symmetry of the C–^{2}H and Ru–^{2}H bonds. Note that the smaller the quadrupolar coupling constant C_Q, the smaller the size of the ellipsoid in that kind of representation.

3.3 Tp* ruthenium complexes

All values calculated for C_Q, η_Q and $\Delta\nu_Q$ employing the cc-pVTZ basis set are given in Table 3. Owing to the presence of fast molecular vibrations, which cause slight reductions of the experimental quadrupolar splittings for C–D, they are found to be in the range of 120–145 kHz. Since the theoretical calculations are performed for 0 K, the calculated values are typically in a more narrow range, with $\Delta\nu_Q$ values close to 142–145 kHz for all complexes, independent of the ligand.

According to our calculations, the quadrupolar splitting of the deuteron bonded to the boron of the Tp* ligand (B–D) should be observed at ~95 kHz. Since no noticable Pake pattern with this quadrupolar splitting was found in the experimental spectra,[17] we conclude that the large distance between the deuterons bonded directly to the ruthenium atom (Ru–D) and the hydrogen bonded to the boron of the Tp*

Table 2 Comparison of the basis sets effect on the ^{2}H NMR parameters (C_Q (in kHz), $\Delta\nu_Q$ (in kHz) and η_Q) for mononuclear Cp* ruthenium complex. The experimental parameters were extracted from the ^{2}H spectra of the complex measured at 90 K.[17] All average bond lengths (*R*) are given in Å

Basis set	6-31G(*d,p*)			6-311G(*d,p*)			cc-pVTZ				Experimental	
Parameters	C_Q	$\Delta\nu_Q$	η_Q	C_Q	$\Delta\nu_Q$	η_Q	*R*	C_Q	$\Delta\nu_Q$	η_Q	$\Delta\nu_Q$	η_Q
C–D (Me)	196	147	0.04	203	152	0.03	1.094	191	143	0.03	—	—
Ru–D	110	82	0.04	109	82	0.05	1.587	97	73	0.07	70	0.09
C–D (Ph)	202	151	0.07	210	157	0.06	1.087	196	147	0.06	—	—

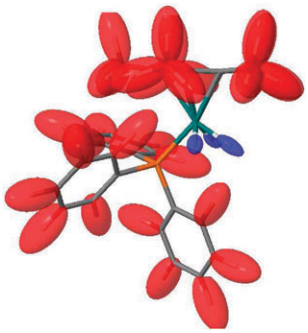

Fig. 4 EFG tensors at ^{2}H centers for Cp*RuD$_3$(PPh$_3$). The EFG tensors of hydrides are plotted in blue for visual convenience.

Table 3 C_Q (in kHz), $\Delta\nu_Q$ (in kHz) and η_Q values for several mononuclear Tp* ruthenium complexes. Comparison between theoretical (cc-pVTZ basis set) and experimental quadrupolar splitting $\Delta\nu_Q$ and asymmetry parameter η_Q. The experimental parameters were extracted from the ^{2}H spectra of the complexes measured at low temperatures: Tp*RuD(THT)$_2$ at 170 K, Tp*RuD(D$_2$)(THT) at 150 K and Tp*RuD(D$_2$)$_2$ at 10 K.[17] All bond lengths (R) are given in Å

	Theoretical calculations				Experimental	
Parameters	R	C_Q	$\Delta\nu_Q$	η_Q	$\Delta\nu_Q$	η_Q
Tp*RuD(THT)$_2$						
C–D (TP*)	1.094	193	145	0.03	120	0.06
C–D(THT)	1.093	189	142	0.01	120	0.06
B–D	1.200	126	95	0.00	—	—
Ru–D	1.603	88	66	0.03	70	0.00
Tp*RuD(D$_2$)(THT)						
C–D (TP*)	1.094	194	145	0.03	126	0.00
C–D (THT)	1.093	189	142	0.02	126	0.00
B–D	1.200	127	95	0.00	—	—
Ru–D	1.597	92	69	0.02	66	0.06
Ru–(D$_2$)	1.619	86	64	0.24	40	0.10
	1.582	97	73	0.08	40	0.10
R_{DD}		1.066				
R_{Ru-D_2}		1.518				
Tp*RuD(D$_2$)$_2$						
C–D (Tp*)	1.094	193	145	0.04	144	0.06
B–D	1.200	127	95	0.00	—	—
Ru–D	1.599	92	69	0.01	68	0.08
Ru–(D$_2$)[a]	1.663	73	55	0.92	42	0.05
	1.639	75	56	0.82	42	0.05
Ru–(D$_2$)[a]	1.664	73	55	0.93	42	0.05
	1.639	74	56	0.83	42	0.05
R_{DD}		0.940/0.941				
R_{Ru-D_2}		1.583/1.583				

[a] These two entries correspond to each of the two D$_2$ subunits.

ligand (B–H) efficiently inhibits the hydrogen/deuteron exchange between Ru–D and B–H.

As can be seen in Table 3, Ru–D bond lengths in Tp* ruthenium complexes are similar to those observed in the previous Cp* ruthenium complex. The quadrupolar splitting calculated for Ru–D therefore is nearly the same for all complexes, with values in the range of 65–69 kHz, similarly to the experimental values.

A discrepancy seems to occur in the case of D$_2$ coordinated to ruthenium, which appears in Tp*RuD(D$_2$)(THT) and Tp*RuD(D$_2$)$_2$ (Fig. 3b and c). While according to our calculations $\Delta\nu_Q$ is expected to be observed at $\approx$55 kHz for Tp*RuD(D$_2$)$_2$ and $\approx$73 kHz for Tp*RuD(D$_2$)(THT), experiments exhibit a splitting close to 40 kHz. Actually, this apparent disagreement is related to the fast rotation of D$_2$ ligands which is not frozen in the temperature range of the experiments, *i.e.* from 10 K to 170 K, whereas calculations correspond to the 0 K limit. This explanation is confirmed by the experimental work of Wehrmann *et al.*[52] who performed low temperature ^{2}H solid-state NMR measurements at 5.4 K at the *trans*-[Ru(D$_2$)Cl(PPh$_2$CH$_2$CH$_2$PPh$_2$)$_2$]$^+$PF$_6^-$ complex, which also includes a D$_2$ ligand however with relatively high rotational barrier of the D$_2$ rotation (6.2 kcal mol^{-1} according to experiments). Here the measured quadrupolar splitting $\Delta\nu_Q$ of the D$_2$ at temperatures below 10 K is close to 60 kHz, *i.e.* the typical theoretical value calculated for η^2-D$_2$ ligands. In the case of the ruthenium complexes considered in this work, the calculated barriers of rotation are much lower (for example ΔE = 2.5 kcal mol^{-1}; $\Delta_r G^\circ$ = 2.2 kcal mol^{-1} for Tp*RuD(D$_2$)(THT)). This confirms that the D$_2$ ligands are in fast rotation in these complexes. The calculation of $\Delta\nu_Q$ (Table 4) of the cation structure *trans*-[Ru(D$_2$)Cl(PPh$_2$CH$_2$CH$_2$PPh$_2$)$_2$]$^+$ (Fig. 5) yielded a value of $\Delta\nu_Q \approx$ 55 kHz which is as expected in good agreement with the experimental one. This theoretical value coincides well with the theoretical $\Delta\nu_Q$ values of the dihydrogen ligands in these complexes (55–75 kHz). This corroborates our interpretation of the low experimental quadrupolar splitting values for D$_2$ in the Tp* as a dynamic effect. It is important to note in this context that the rotation of the D$_2$ ligands is an exact quantum mechanical symmetry operation, which occurs at low temperatures as a tunnel process and as a conventional chemical exchange process at higher temperatures. For a detailed discussion see the reviews ref. 14 and 15.

Table 4 C_Q (in kHz), $\Delta\nu_Q$ (in kHz) and η_Q values calculated for the *trans*-[Ru(D$_2$)Cl(PPh$_2$CH$_2$CH$_2$PPh$_2$)$_2$]$^+$ cation. Comparison between theoretical (cc-pVTZ basis set)[a] and experimental quadrupolar splitting $\Delta\nu_Q$ and asymmetry parameter η_Q. The experimental parameters were extracted from the ^{2}H spectra of the *trans*-[Ru(D$_2$)Cl(PPh$_2$CH$_2$CH$_2$PPh$_2$)$_2$]$^+$PF$_6^-$ complex measured at 5.4 K[52]

	Theoretical calculations				Experimental	
Parameters	R	C_Q	$\Delta\nu_Q$	η_Q	$\Delta\nu_Q$	η_Q
C–D (CH)	1.086	197	147	0.07	—	—
C–D (CH$_2$)	1.094	186	140	0.03	—	—
Ru–(D$_2$)	1.632	73	55	0.96	60	0
	1.636	73	55	0.96	60	0
R_{DD}		0.945				

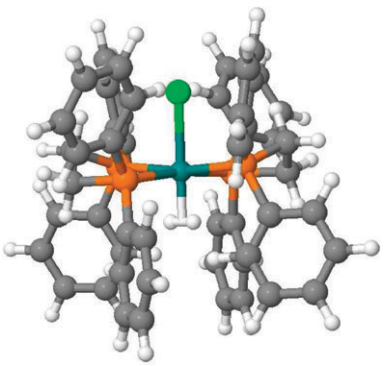

Fig. 5 Optimized cation structure of the *trans*-[Ru(D$_2$)Cl(PPh$_2$CH$_2$CH$_2$PPh$_2$)$_2$]$^+$PF$_6^-$ complex.

The D–D bond lengths are also reported in Table 3. The D_2 ligand is significantly more elongated in Tp*RuD(D_2)(THT) with respect to Tp*RuD(D_2)$_2$, owing to the more important back-donation in the σ^* molecular orbital of H_2. As a consequence $\Delta\nu_Q$ tends to the typical value for terminal deuterons, *i.e.* 65–70 kHz. One should pay attention to the asymmetry parameter η_Q. According to experiments it typically ranges from 0 to 0.1 for deuterium, even in the case of η^2-D_2 ligands. While we also find small asymmetry parameters for Ru–H bonds, η_Q is systematically found to be close to 1 for deuterium atoms involved in Ru–D_2 bonding, with the exception of Tp*RuD(D_2)(THT). According to eqn (5), such a situation arises when similar values are obtained for V_{22} and V_{33}, whereas $V_{11} \sim 0$. While this seems very unusual for D atoms, this must be related to the specific bonding of η^2-D_2 ligands. As a matter of fact, small values of the asymmetry parameter indicate a weak deviation from the cylindrical symmetry in the H–X bond. This symmetry is broken in Ru–D_2 complexes in so far as D is involved both in Ru–D and D–D bonding. We have checked by optimizing Tp*RuD(D_2)$_2$ within the cc-pvtz/Stuttgart basis set that this is not an artefact related to an inconsistency of basis sets between the optimization process and the EFG calculation. At the moment it is not clear why the calculated asymmetry is so high.

3.4 PCy_3 ruthenium complex

The calculated C_Q, $\Delta\nu_Q$ and η_Q values for the $RuD_2(D_2)_2(PCy_3)_2$ complex depicted in Fig. 3e are summarized in Table 5. While the $\Delta\nu_Q$ values calculated for Ru–D agree well with the experimental ones (70 and 68 kHz *vs.* 66 kHz), the $\Delta\nu_Q$ values for Ru–D_2 are again overestimated with respect to experiments ($\approx$60 kHz *vs.* 42 kHz), whereas η_Q is close to 1, as already calculated in the previous ruthenium dihydrides. This phenomenon also refers to the fast rotation of the D_2 as it is explained before.

In agreement with the experimental findings, the calculations reveal that $\Delta\nu_Q$ for Ru–D is not sensitive to the type of ligands nor to the number of deuterons coordinated to the ruthenium. Ru–D bond lengths in the PCy_3 complex and in Tp* complexes differ at most by 0.015 Å, which has a weak impact on $\Delta\nu_Q$. Considering the particularly short D–D bond length (0.88 Å), a lower value for $\Delta\nu_Q$ was expected. However D_2 is significantly farther from the Ru center in the $RuD_2(D_2)_2(PCy_3)_2$ than in the Tp* complexes, which may explain the high theoretical $\Delta\nu_Q$ value.

Table 5 C_Q (in kHz), $\Delta\nu_Q$ (in kHz) and η_Q values for $Ru(D)_2(D_2)_2(PCy_3)_2$. Experimental values were obtained at 60 K.[17] All bond lengths (R) are given in Å

	Theoretical calculations				Experimental	
Parameters	R	C_Q	$\Delta\nu_Q$	η_Q	$\Delta\nu_Q$	η_Q
C–D	1.096	186	140	0.02	122	0.04
Ru–D	1.604	93	70	0.03	66	0.10
Ru–D	1.612	91	68	0.02	66	0.10
Ru–$(D_2)^A$	1.751	81	60	0.86	42	0.01
	1.717	76	57	0.99	42	0.01
Ru–$(D_2)^B$	1.728	80	60	0.94	42	0.01
	1.755	83	62	0.85	42	0.01
R_{DD}		0.877/0.882				
R_{Ru-D_2}		1.685/1.677				

4. Conclusion

In this work ^{2}H solid-state NMR quadrupolar interactions of deuterons in five ruthenium organometallic complexes have been studied by DFT methods. It was shown that the variation of the size of the basis set has no significant influence on the quadrupolar splittings $\Delta\nu_Q$ and asymmetry parameters η_Q, although the best agreement between calculated and experimental data is obtained with the cc-pVTZ basis set. In general a quasi-systematic overestimation of the quadrupolar coupling constant C_Q is found, as compared to the experimental values. This might be due to vibrational motions of the X–D groups which cause a partial reduction of the experimental value in the observed temperature region.

This joint theoretical/experimental strategy seems in particular very promising for elucidating the coordination mode of deuterium with metal atoms as well as the origin (Ru–D *vs.* D in ligands) of all the features observed on experimental spectra. As confirmed by DFT calculations, experimental quadrupolar splitting values are different for terminal-deuterium atoms and η^2-dideuterium. However one has to pay attention to temperature effects which may significantly modify experimental quadrupolar splittings. This is the case in dideuterium complexes, due to the rotational motion of D_2. This rotation can be frozen only for few compounds with relatively large D–D distances and correspondingly high rotational barriers. In all other cases the problem has to be solved by calculating the motionally averaged tensor and comparing this value to the experimental tensors, which is feasible by standard solid-state NMR techniques. The main discrepancy between DFT and ^{2}H MAS NMR data lies in the calculation of η_Q for D_2 ligands, since it is experimentally found to be symmetric whereas the theoretical value is close to 1. This disagreement could mean that DFT is ill-suited for the calculation of η_Q in the specific case D_2 ligands, owing to a bad description of the electron density at the nuclei. Nevertheless, if we consider that DFT is right, the difference between the NMR parameters at the rigid limit and the parameters measured below 10 K could mean that there is a second faster motional process in addition to the experimentally observed tunneling, which does a preaveraging of the calculated asymmetric tensor to the relatively symmetric tensor which is observed in the low-temperature ($<$10 K) solid-state NMR spectra. It deserves further theoretical work, using advanced molecular dynamics methods.

In conclusion, the combination of our experimental study and our quantum chemical calculations opens the road for a structural interpretation of deuterium quadrupolar coupling constants in transition metal nanoparticles. The next step on this road is the experimental and theoretical study of the coordination of hydrides in more complex species, such as oligonuclear complexes or organometallic clusters. Such compounds exhibit a larger variety of coordination modes (terminal, edge-bridging, face-capping) which can also be encountered at the surface of nanoparticles. This will be the topic of a forthcoming paper.

Acknowledgements

Financial support by the Deutsche Forschungsgemeinschaft under contract Bu-911/12-1, the CNRS and the ANR (SIDERUS project, ANR-08-BLAN-0010-03 and ANR-08-BLAN-0010-04) is gratefully acknowledged. Torsten Gutmann thanks the Federal State of Thuringia for a PhD Scholarship. We also thank the CALcul en MIdi-Pyrénées (CALMIP) for generous allocations of computer time. Laurent Maron is a member of the Institut Universitaire de France (IUF).

References

1 G. C. Bond, B. Coq, R. Dutartre, J. Garcia Ruiz, A. D. Hooper, M. Grazia Proietti, M. C. Sanchez Sierra and J. C. Slaa, *J. Catal.*, 1996, **161**, 480–494.
2 C. Six, K. Beck, A. Wegner and W. Leitner, *Organometallics*, 2000, **19**, 4639–4642.
3 P. M. Maitlis, *J. Organomet. Chem.*, 2004, **689**, 4366–4374.
4 M. W. McQuire and C. H. Rochester, *J. Catal.*, 1995, **157**, 396–402.
5 *Clusters and Colloids: From Theory to Applications*, ed. G. Schmid, VCH Publishers, Inc., Weinheim, Germany, 1994.
6 *Nanoscale Materials in Chemistry*, ed. K. J. Klabunde, Wiley-Interscience, New-York, 2001.
7 *Nanoparticles. From Theory to Application*, ed. G. Schmid, Wiley-VCH, Weinheim, Germany, 2004.
8 A. Adamczyk, Y. Xu, B. Walaszek, F. Roelofs, T. Pery, K. Pelzer, K. Philippot, B. Chaudret, H.-H. Limbach, H. Breitzke and G. Buntkowsky, *Top. Catal.*, 2008, **48**, 75–83.
9 W. P. Halperin, *Rev. Mod. Phys.*, 1986, **58**, 533–606.
10 P. Ménini, F. Parret, M. Guerrero, K. Soulantica, L. Erades, A. Maisonnat and B. Chaudret, *Sens. Actuators, B*, 2004, **103**, 111.
11 G. Buntkowsky, H.-H. Limbach, F. Wehrmann, I. Sack, H. M. Vieth and R. H. Morris, *J. Phys. Chem. A*, 1997, **101**, 4679.
12 G. Facey, D. Gusev, S. Macholl, R. H. Morris and G. Buntkowsky, *Phys. Chem. Chem. Phys.*, 2000, **2**, 935.
13 F. Wehrmann, J. Albrecht, E. Gedat, G. J. Kubas, H. H. Limbach and G. Buntkowsky, *J. Phys. Chem. A*, 2002, **106**, 2855.
14 G. Buntkowsky and H. H. Limbach, *Dihydrogen transfer and symmetry: The role of symmetry on the chemistry of dihydrogen transfer in the light of nmr spectroscopy*, in *Hydrogen-Transfer Reactions*, ed. J. P. Hynes, J. P. Klinman, H. H. Limbach and R. L. Schowen, Wiley-VCH, Weinheim, 2006, vol. 2, pp. 639–682.
15 G. Buntkowsky and H. H. Limbach, *J. Low Temp. Phys.*, 2006, **143**, 55–114.
16 F. Schroeder, D. Esken, M. Cokoja, M. W. E. van den Berg, O. I. Lebedev, G. van Tendeloo, B. Walaszek, G. Buntkowsky, H.-H. Limbach, B. Chaudret and R. A. Fischer, *J. Am. Chem. Soc.*, 2008, **130**, 6119–6130.
17 B. Walaszek, A. Adamczyk, T. Pery, X. Yeping, T. Gutmann, N. de S. Amadeu, S. Ulrich, H. Breitzke, H. M. Vieth, S. Sabo-Etienne, B. Chaudret, H.-H. Limbach and G. Buntkowsky, *J. Am. Chem. Soc.*, 2008, **130**, 17502–17508.
18 S. Macholl, F. Börner and G. Buntkowsky, *Z. Phys. Chem.*, 2003, **217**, 1473–1505.
19 J. Autschbach, *Density Functional Theory in Inorganic Chemistry*, volume 112 of *Structure and Bonding*, chapter: The Calculation of NMR Parameters in Transition Metal Complexes, Springer-Verlag, Berlin/Heidelberg, 2004, pp. 1–48.
20 I. del Rosal, L. Maron, R. Poteau and F. Jolibois, *Dalton Trans.*, 2008, 3959–3970.
21 I. del Rosal, F. Jolibois, L. Maron, K. Philippot, B. Chaudret and R. Poteau, *Dalton Trans.*, 2009, 2142–2156.
22 A. Schweitzer, T. Gutmann, M. Wächtler, H. Breitzke, A. Buchholz, W. Plass and G. Buntkowsky, *Solid State Nucl. Magn. Reson.*, 2008, **34**, 52–67.
23 L. Truflandier, M. Paris, C. Payen and F. Boucher, *J. Phys. Chem. B*, 2006, **110**, 21403–21407.
24 T. Gutmann, A. Schweitzer, M. Wächtler, H. Breitzke, A. Buchholz, W. Plass and G. Buntkowsky, *Z. Phys. Chem.*, 2008, **222**, 1389–1406.
25 F. Jolibois, O. Soubias, V. Réat and A. Milon, *Chem.–Eur. J.*, 2004, **10**, 5996–6004.
26 O. Soubias, F. Jolibois, V. Réat and A. Milon, *Chem.–Eur. J.*, 2004, **10**, 6005–6014.
27 M. Mirzaei, N. L. Hadipour and K. Ahmadi, *Biophys. Chem.*, 2007, **125**, 411–415.
28 Daniel Sebastiani and Michele Parrinello, *Dalton Trans.*, 2002, **3**, 675–679.
29 C. Raynaud, L. Maron, J.-P. Daudey and F. Jolibois, *ChemPhysChem*, 2006, **7**, 407–413.
30 W. C. Bailey, *J. Mol. Spectrosc.*, 1998, **190**, 318–323.
31 E. Gedat, A. Schreiber, J. Albrecht, T. Emmler, I. Shenderovich, G. H. Findenegg, H.-H. Limbach and G. Buntkowsky, *J. Phys. Chem. B*, 2002, **106**, 1977–1984.
32 W. Hoffmann, G. Buntkowsky and H.-M. Vieth, *Appl. Magn. Res.*, 1999, **17**, 489–502.
33 B. Moreno, S. Sabo-Etienne, B. Chaudret, A. Rodriguez, F. Jalon and S. Trofimenko, *J. Am. Chem. Soc.*, 1995, **117**, 7441–7451.
34 K. Schmidt-Rohr and H. W. Spiess, *Multidimensional Solid-State NMR and Polymers*, chapter Principles of NMR of Organic Solids, Academic Press Inc, 1994, pp. 13–68.
35 P. Pykkö, *Mol. Phys.*, 2001, **99**, 1617–1629.
36 C_Q and $\Delta\nu_Q$ are often written as Q_{cc} and Q_{zz}.
37 M. J. Frisch, G. W. Trucks, H. B. Schlegel, G. E. Scuseria, M. A. Robb, J. R. Cheeseman, J. A. Montgomery, Jr., T. Vreven, K. N. Kudin, J. C. Burant, J. M. Millam, S. S. Iyengar, J. Tomasi, V. Barone, B. Mennucci, M. Cossi, G. Scalmani, N. Rega, G. A. Petersson, H. Nakatsuji, M. Hada, M. Ehara, K. Toyota, R. Fukuda, J. Hasegawa, M. Ishida, T. Nakajima, Y. Honda, O. Kitao, H. Nakai, M. Klene, X. Li, J. E. Knox, H. P. Hratchian, J. B. Cross, V. Bakken, C. Adamo, J. Jaramillo, R. Gomperts, R. E. Stratmann, O. Yazyev, A. J. Austin, R. Cammi, C. Pomelli, J. Ochterski, P. Y. Ayala, K. Morokuma, G. A. Voth, P. Salvador, J. J. Dannenberg, V. G. Zakrzewski, S. Dapprich, A. D. Daniels, M. C. Strain, O. Farkas, D. K. Malick, A. D. Rabuck, K. Raghavachari, J. B. Foresman, J. V. Ortiz, Q. Cui, A. G. Baboul, S. Clifford, J. Cioslowski, B. B. Stefanov, G. Liu, A. Liashenko, P. Piskorz, I. Komaromi, R. L. Martin, D. J. Fox, T. Keith, M. A. Al-Laham, C. Y. Peng, A. Nanayakkara, M. Challacombe, P. M. W. Gill, B. G. Johnson, W. Chen, M. W. Wong, C. Gonzalez and J. A. Pople, *GAUSSIAN 03 (Revision B.05)*, Gaussian, Inc., Wallingford, CT, 2004.
38 C. Adamo and V. Barone, *J. Chem. Phys.*, 1999, **110**, 6158–6170.
39 L. L. Wang and D. D. Johnson, *J. Phys. Chem. B*, 2005, **109**, 23113–23117.
40 W. Küchle, M. Dolg, H. Stoll and H. Preuss, *Mol. Phys.*, 1991, **74**, 1245–1263.
41 P. C. Harihara and J. A. Pople, *Theor. Chem. Acc.*, 1973, **28**, 213–222.
42 W. J. Hehre, R. Ditchfield and J. A. Pople, *J. Chem. Phys.*, 1972, **56**, 2257–2261.
43 A. D. Becke, *J. Chem. Phys.*, 1993, **98**, 5648–5652.
44 K. Burke, J. P. Perdew and Y. Wang, *Electronic Density Functional Theory: Recent Progress and New Directions*, chapter Derivation of a Generalized Gradient Approximation: the PW91 Density Functional, Plenum, New York, 1998.
45 J. P. Perdew, chapter Unified Theory of Exchange and Correlation Beyond the Local Density Approximation, *Electronic Structure of Solids*, Akademie, Berlin, 1991.
46 J. P. Perdew, J. A. Chevary, S. H. Vosko, K. A. Jackson, M. R. Pederson, D. J. Singh and C. Fiolhais, *Phys. Rev. B: Condens. Matter Mater. Phys.*, 1992, **46**, 6671.
47 J. P. Perdew, J. A. Chevary, S. H. Vosko, K. A. Jackson, M. R. Pederson, D. J. Singh and C. Fiolhais, *Phys. Rev. B: Condens. Matter Mater. Phys.*, 1993, **48**, 4978.
48 J. P. Perdew, K. Burke and Y. Wang, *Phys. Rev. B: Condens. Matter Mater. Phys.*, 1996, **54**, 16533.
49 J. P. Perdew, Kieron Burke and Yue Wang, *Phys. Rev. B: Condens. Matter Mater. Phys.*, 1998, **57**(23), 14999.
50 E. R. Davidson, *Chem. Phys.*, 1996, **260**, 514–518.
51 D. E. Woon and T. H. Dunning, *J. Chem. Phys.*, 1993, **98**, 1358–1371.
52 F. Wehrmann, T. P. Fong, R. H. Morris, H.-H. Limbach and G. Buntkowsky, *Phys. Chem. Chem. Phys.*, 1999, **1**, 4033–4041.